Chemical Science

ROYAL SOCIETY OF CHEMISTRY

EDGE ARTICLE

View Article Online
View Journal | View Issue

Cite this: *Chem. Sci.*, 2020, **11**, 11468

All publication charges for this article have been paid for by the Royal Society of Chemistry

Received 27th July 2020
Accepted 28th September 2020

DOI: 10.1039/d0sc04098c

rsc.li/chemical-science

Phase transfer of metal cations by induced dynamic carrier agents: biphasic extraction based on dynamic covalent chemistry†

Aline Chevalier,[ab] Artem Osypenko,[b] Jean-Marie Lehn *[b] and Daniel Meyer*[a]

In contrast to the classical method where a single molecule is designed to extract metal cations under specific conditions, dynamic covalent chemistry provides an approach based on the implementation of an adaptive dynamic covalent library for inducing the generation of the extractant species. This approach has been applied to the liquid–liquid extraction of copper(II) nitrate based on a dynamic library of acylhydrazones constituents that self-build and distribute through the interface of a biphasic system. The addition of copper(II) cations to this library triggers a modification of its composition and the up-regulation of the ligand molecules driven by coordination to the metal cations. Among these, one species has proven to be sufficiently lipophilic to play the role of carrier agent and its formation by component exchange enables the partial extraction of the copper(II). The study of different pathways to generate the dynamic covalent library demonstrates the complete reversibility and the adaptability of the system. The detailed analytical investigation of the system provides a means to assess the mechanism of the dynamic extraction process.

Introduction

Solving a liquid–liquid metal extraction problem is usually based on a "one problem–one solution" approach. For a given problem such as that raised by treatment of spent nuclear fuel,[1] mining of minerals[2] or any other metal extraction procedure,[3] liquid–liquid extraction offers a molecular system that can be designed, synthesised, characterised and studied under various conditions. Usually, the nature of any study is highly specific and depends upon the composition of the aqueous phase in regard to the metal cations, their counter-anions and the acidity. The properties of such an extraction system for a given aqueous phase depend strongly on the water-immiscible organic solvent and the molecular extractant as a pair.‡ In order to be able to extract a metal cation from an aqueous phase and carry it into an organic phase, the extractant molecule must have three main characteristics: (i) strong and selective complexation of metal cations, (ii) organic phase solubility and (iii) limited aqueous solubility.

The properties of an extracting system can be modified in several ways with or without changing the molecular complexation agent itself. The type of modification performed depends upon the relative importance of the different interactions as driving forces for the liquid–liquid extraction of specific metallic species. The easiest modification lies in the reformulation of the extractant–solvent pair.‡ Nevertheless, if the extracting molecule needs to be modified, two approaches may be considered: (i) keeping the metal complexing site unchanged while modifying other molecular features, or (ii) opting for a total modification of the extractant. In the first case, variation of the properties, such as that of lipophilicity, is mainly ruled by the physicochemical features resulting from the interactions with the medium. In the second case, modifying the complexing pattern of the extracting molecule will drastically change the direct metal–ligand interactions with a marked effect on the behaviour of the system.

As the reformulation and molecular structural modifications primarily concern weak interactions between the metal complex and the molecules in the organic phase, a proper understanding of these relationships is essential when considering the liquid–liquid extraction of metal.[4] In general, the organic molecular connectivity remains the same during a liquid–liquid extraction of metal cations because the molecules are covalently built, that is to say, "static", thus preventing any major change in their interactions. In strong contrast, the Dynamic Covalent Chemistry approach (DCC)[5] allows for *in situ* variations in molecular constitution by component exchange and recombination induced in an adaptive fashion by the system itself.

[a]*Institut de Chimie Séparative de Marcoule (ICSM), CEA, CNRS, ENSCM, Université de Montpellier, UMR 5257, Bâtiment 426, BP 17171, 30207 Bagnols-sur-Cèze, France. E-mail: daniel.meyer@cea.fr*

[b]*Laboratoire de Chimie Supramoléculaire, Institut de Science et d'Ingénierie Supramoléculaires (ISIS), UMR 7006, 8 Allée Gaspard Monge, 67000 Strasbourg, France. E-mail: lehn@unistra.fr*

† Electronic supplementary information (ESI) available. CCDC 2014872–2014874. For ESI and crystallographic data in CIF or other electronic format see DOI: 10.1039/d0sc04098c

It implements reversible chemical reactions within sets of initial components to generate dynamic constitutional diversity and gives access to Dynamic Covalent Libraries (DCLs). DCC relies on the reversible and continuous formation and cleavage of chemical bonds so as to generate the constituents consisting of all possible combinations obtained by exchange of their components. The resulting distribution can undergo spontaneous modifications in response to a physical stimulus or a chemical effector such as metalloselection,[6] photoselection[7] or kinetic and thermodynamic changes.[8] DCLs thus display adaptive behaviour in response to the environment/medium and the applied agents.

The use of binary liquid mixtures enables the examination of the behaviour of a DCL in a phase separation process.[9] The dynamic library adapts to the phase separation and undergoes a constitutional reorganisation generating a distribution of the fittest constituents for each phase. Component exchange across the interface between the separated liquid layers is markedly slowed down and depends on the phase affinities of the different components. Thus, the system may be kinetically blocked in an out-of-equilibrium distribution.[10] When the phases are re-united into a single phase, the dynamic library returns to its initial equilibrium state, thus displaying the full reversibility of the system. Phase transfer of multiple metal cations leads to the generation of cation specific distributions.[11]

In the present work, the structural, kinetic and thermodynamic features of several DCLs have been explored in order to define the parameters and conditions required for achieving suitable constituent formation and distribution as well as dynamic covalent exchanges of component across the interface. The dynamism of the implemented libraries takes place at different level: (i) formation and exchange of C=N bonds; (ii) metal/ligand exchange; (iii) phase transfer; (iv) protonation/deprotonation of the ligands.

Most significantly, the addition of a metal salt to the DCLs triggers the redistribution within as well as between both phases of the components, the ligand constituents and the corresponding complexes depending on the nature of the added chemical effector. The present systems are thus adaptive, responding to a specific metal cation and allowing for its transfer from an aqueous phase to an organic phase. Such a behaviour has been implemented for the extraction of Zn(II) or Cd(II) ions by means of a dynamic combinatorial Schiff-base library.[12]

The DCL-based approach introduces a new paradigm in the liquid–liquid extraction–separation field because intrinsic chemical modifications occur in the system during the extraction process. Indeed, the interactions and their consequences are not frozen but add dynamic degrees of freedom that offer additional opportunities to study the importance of the strong–weak interactions in metal extraction in biphasic systems. More specifically, the work reported here describes the adaptive behaviour of DCLs based on aldehyde/hydrazide components and their tridentate acylhydrazone ligand constituents in the process of inducing copper(II) phase transfer from an aqueous phase to an organic phase. It represents an exploration of the fundamentals of dynamic covalent chemistry as applied to liquid–liquid extraction. The main goal is the selective transfer of metals from one phase to another in a non-miscible biphasic system.[13]

Results and discussion

Choice of the DCL components and of experimental extraction conditions

Components. The overall features of acylhydrazones[14] make them good candidates for an adaptive extracting molecular system.[12b] They can be easily obtained by condensation between an aldehyde and a hydrazide and they can undergo reversible transhydrazination (Scheme 1). Their dynamic covalent behaviour has been studied in a number of cases.[6b,7b,9b,12b,15] The hydrophobic–hydrophilic exchange behaviour, the strength of the complexation properties and the susceptibility to ionization of acylhydrazone can be regulated through the nature of the $R_{1\rightarrow4}$ and X groups (X = H or CH_3).

Based on complexation and solubility properties, the presence of a deprotonatable site and hydrophilic–hydrophobic properties, 16 aldehydes and 4 hydrazides were identified as potential components (Fig. S17 in ESI†). The four hydrazides **B1–B4** were chosen as they span a range of lipo-hydrophilic balance, the more lipophilic, **B2**, being a good candidate for extraction into an organic phase (Fig. 1). From a first series of formation tests based on the reactivity of **B2** with the 16 aldehydes, only 10 gave the acylhydrazone in the present conditions.

As the present work is mainly focused on the role played by a labile proton and the hydrophobic–hydrophilic balance, the two aldehydes **A1** and **A2** were mainly considered. **A3** as structural analogue of **A1** and **B3** as an analogue of **B4** were used only in the study of kinetic features. Altogether, the final set of

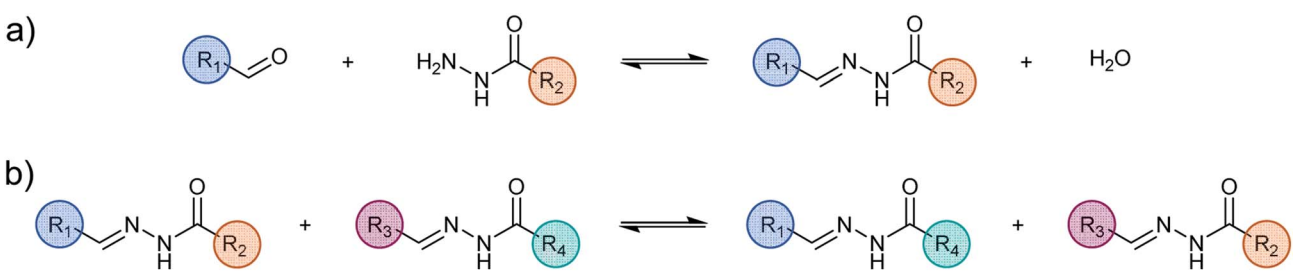

Scheme 1 (a) Reaction of formation (b) reaction of exchange of acylhydrazone.

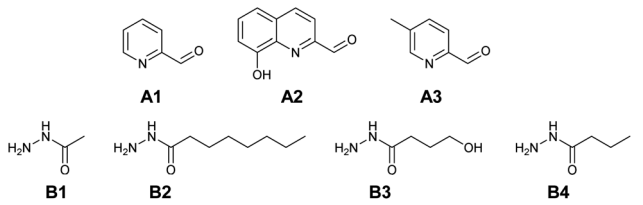

Fig. 1 Reference library of aldehyde **A1–A3** and hydrazide **B1–B4** components.

molecules **A1–A3** and **B1–B4** forms the reference library used here (Fig. 1).

Conditions. The pK_a of the acylhydrazones make pH an important parameter for the liquid–liquid extraction of metals. The simulations of the pK_a of **HA1B1** and **HA1B2** estimate the p$K_{a1} = 3.2$ and 3 respectively and p$K_{a2} = 11.8$. The titrations of the complexes [Cu(II)(**HA1B1**)$_2$] and [Cu(II)(**HA1B2**)$_2$] by sodium hydroxide gives respectively p$K_{a1} = 3.1$ and 2.2 and p$K_{a2} = 5.3$ and 6. (Fig. S21–S23 in ESI†). Considering these values, it is reasonable to keep the pH above 2. Moreover, precipitation of metals salt is observed at pH > 9.

Qualitative screening of the extraction of Cu(II) in water/organic systems was conducted for chloroform, dichloromethane, toluene, dodecane, 1-octanol and nitromethane. All the solvents showed, by direct observation, a similar behaviour towards Cu(II) extraction by the ligands formed by the reference library (Fig. S18 and S19 in ESI†). Chloroform was chosen for further investigations, as it presents balanced solubilisation properties and is easily available in deuterated form for extraction experiments monitored by ^{1}H nuclear magnetic resonance spectroscopy (NMR).

Extraction test experiments. The metal cation extraction properties were studied for the acylhydrazones produced by the reference library. In addition, the important role played by the ionizable N–H proton was established by comparing the properties of some of the N–H constituents **HAaBb**§ with those of their *N*-methylated analogues **Me-AaBb** (Fig. 2; see Section 2 of ESI† for synthesis and characterisation details).

The extraction experiments were conducted by introducing the studied ligand constituent into a H_2O : $CHCl_3$ (1 : 1, v/v) biphasic system and stirring until equilibration at room temperature. Then 0.5 equivalent of Cu(II) was added and the system was stirred for one hour. The electronic absorptions were recorded and exhibited new peaks in the visible region for the N–H acylhydrazones (Fig. S24–S27 in ESI†), whereas the spectra of the corresponding *N*-methylated derivatives did not show any such peaks. The occurrence of these peaks is consistent with the formation of a complex of the NH acylhydrazone and Cu(II). The coordination involves the carbonyl-O, the imine-N and the pyridine-N atoms.

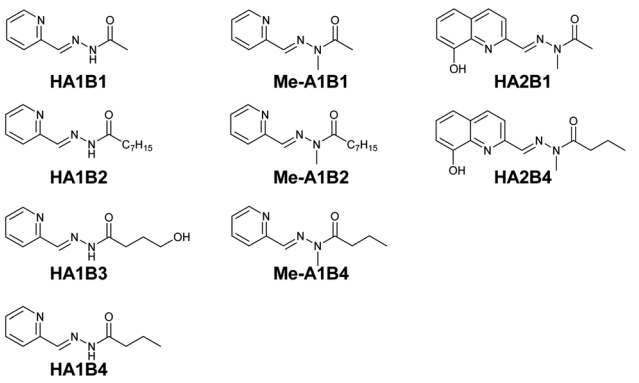

Fig. 2 Acylhydrazone ligand constituents studied in the preliminary extraction tests with $Cu(NO_3)_2 \cdot 3H_2O$.

The effect of the chain length was studied using **A1** and the hydrazides with different carbon chain lengths: CH_3, C_7H_{15} and C_3H_7 for **HA1B1**, **HA1B2** and **HA1B4** respectively. The absorption band of the coordination complex of Cu(II) with **HA1B1** was present in the spectrum of the aqueous phase only (Fig. S24 in ESI†). With **HA1B4** (propyl chain), the peak was visible in the two phases. Assuming identical molar extinction coefficients in water and chloroform, the distribution of the complex [Cu(II)(**HA1B4**)$_2$](NO$_3$)$_2$ is 75 : 25% (aqueous : organic) (Fig. S27 in ESI†). For **HA1B2** (heptyl chain), the aqueous phase stayed colourless and the organic phase turned green due to the presence of the complex in the organic phase (Fig. S26 in ESI†).

Behaviour of the DCLs

Before starting the metal extraction study, the behaviour of the acylhydrazones and the exchange processes within the library were characterised experimentally in one- and two-phase systems. The reactions were run at room temperature (23 °C) at 20 mM in $CDCl_3$ and D_2O at various pD values and monitored by ^{1}H NMR spectroscopy.

For the biphasic studies, the initial distributions of the components and constituents between D_2O and $CDCl_3$ were determined at pD = 6 with an error of ±5%.[16] **A2**, **A3**, **B2**, **HA1B2**, **Me-A1B2** and **Me-A1B4** were dissolved in chloroform (water content below 5%). **B1**, **B3**, and **HA1B3** were dissolved in water (chloroform content below 5%). For the other members of the DCL, the distribution in D_2O : $CDCl_3$ was: **A1** (5 : 95); **B4** (85 : 15); **HA1B1** (40 : 60); **Me-A1B1** (5 : 95); **HA1B4** (13 : 87) (Table S1 in ESI†).

Single phase experiments. The formation and exchange reactions were studied for the **A1** and **A3** aldehydes in single-phase conditions (Scheme 2a). In line with an acid-catalysed mechanism,[17] acylhydrazone formation was faster in water than in chloroform and became faster with decreasing pD (Table 1a) (Fig. S28 in ESI†). To obtain information about the exchange reactions that may occur in actual extraction experiments, three different processes were considered to take place (Scheme 2b–d): exchange 1 between a hydrazide and an acylhydrazone, which may occur *via* aminal formation or *via* hydrolysis and recondensation;[18] exchange 2, between two acylhydrazones involving a hydrolysis mechanism; exchange 3, between a hydrazide and the acylhydrazone ligands on a metal complex.

Like the formation reaction, exchange 1 and exchange 2 are acid catalysed (Table 1b–d; Fig. S29 and S30 in ESI†). The equilibration time of the exchange decreased drastically with pD. In water, the exchange between an acylhydrazone/metal complex

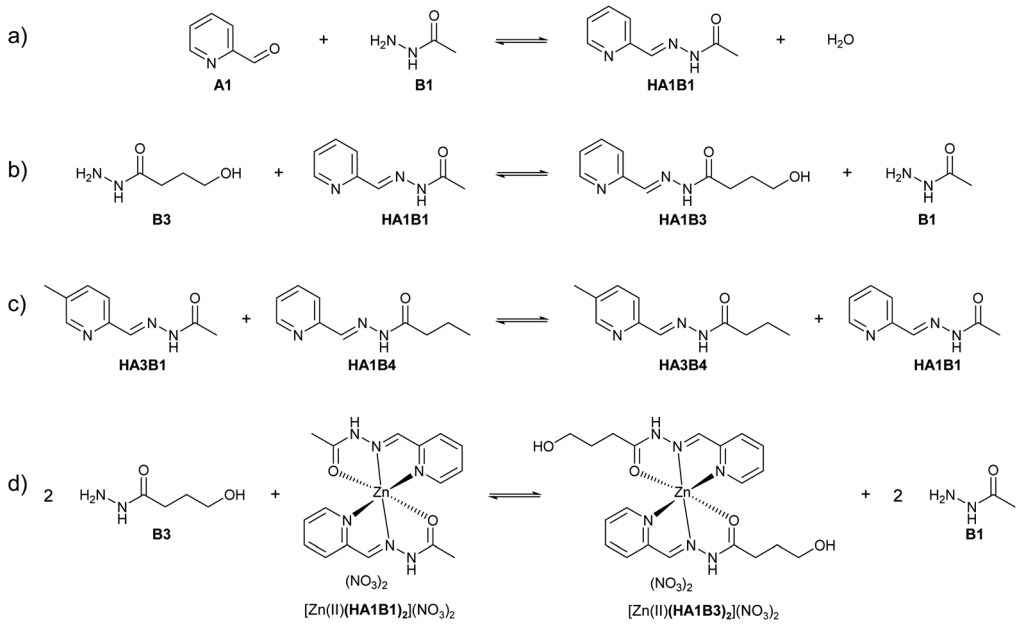

Scheme 2 (a) Reaction of formation of acylhydrazone – types of exchange processes: (b) exchange 1 – between a hydrazide and an acylhydrazone – (c) exchange 2 – between two acylhydrazones – (d) exchange 3 – reaction between a hydrazide and the ligands on a Zn(II) complex.

Table 1 Half-reaction time of formation and equilibration times of exchange reactions in monophasic system (Scheme 2 and Fig. S24–S27 in ESI)

		D_2O		
Reaction	$CDCl_3$	pD = 7	pD = 5	pD = 2.5
(a) Formation	3 h 15	1 h 45	<10 min	<10 min
(b) Exchange 1	—	20 h	2 h	40 min
(c) Exchange 2	—	>3 d	>3 d	24 h
(d) Exchange 3	—	—	5 h	—

and a hydrazide, was made using $[Zn(II)(\mathbf{HA1B1})_2](NO_3)_2$ and **B3**. Zn(II) was used instead of Cu(II) as the two metals have similar Lewis acidity and the reaction is monitored by ^1H NMR spectroscopy. The exchange reached equilibrium within 5 hours at pD = 5 (Fig. S31 in ESI†). Altogether, the single-phase experiments indicated that the rate of component exchange of free and complexed constituents in acidic condition was suitable for extraction processes (Fig. S28–S31 in ESI†).

Biphasic system transphase component exchange. The reaction of **A1** with **B1** or **B2** was studied in a D_2O : $CDCl_3$ system at different pD values of the aqueous phase. As expected, for both acylhydrazones, the reaction was pD dependent and became faster in acidic conditions (Table 2 and Fig. S32 in ESI†).

For the formation of **HA1B2**, solutions of the components **A1** and **B2** were initially introduced into the chloroform phase where the reaction occurs (Fig. S33 in ESI†). The reaction rate increased with the acidity of the water phase in view of the presence of residual water in the wet organic phase (about 0.87 g water per L)[19] (Table 2b).

Comparing the formation reactions at pD = 2.5 shows that acid catalysis greatly increased the reaction rate and there was almost no difference in the formation rates of **HA1B1** and **HA1B2**, both completed within one hour. At pD = 6.3, the formation of **HA1B1** is 4 times faster than the one of **HA1B2**. At pD = 8 **HA1B1** formation is complete within 100 h whereas **HA1B2** reaches 40% of conversion. These comparisons highlight the importance to perform reactions at low pD (Table 2a and b).

Exchange reactions in biphasic conditions were performed on the **HA1B1**/**B2** and **HA1B2**/**B1** sets. At pD 8 and 6, the exchange reactions were slow and raising the temperature to 333 K (60 °C) after one week showed that the thermodynamic equilibrium had not yet been reached (Fig. S34 and S35 in ESI†). As observed previously, the biphasic exchange reactions were

Table 2 Estimated times for reaching equilibrium of formation and exchange reactions in biphasic system (Fig. S28–S32 in ESI)

pD	8	6.3	2.6
(a) **HA1B1** formation	100 h	25 h	<1 h
(b) **HA1B2** formation	Conversion 40% (100 h)	100 h	<1 h
(c) **HA1B1**/**B2** exchange	>3 weeks	10 days	10 h
(d) **HA1B2**/**B1** exchange	>3 weeks	>3 weeks	>3 weeks
(e) **A1**/**B1**/**B2** exchange	>3 weeks	Conversion 80% (10 days)	5 h

catalysed under acidic conditions (Table 2c and d). After one day at pD = 2.5, **HA1B1**/**B2** exchange reached equilibrium and 90% yield whereas the **HA1B2**/**B1** pair did not react (within the 5% estimated error of determination).

When the 3 components **A1**, **B1**, **B2** were mixed at pD 6.3 or 8, the equilibration of formation and component exchange took longer than 100 hours and an increase in temperature from 296 to 333 K had a very limited impact (Table 2e). It is assumed that reaction proceeded by the rapid formation of **HA1B1** in the aqueous phase followed by its transfer to the chloroform phase where the exchange with **B2** occurred (Fig. S36 in ESI†).

Considering the [**A1** + **B1** + **B2**] system, acid catalysis led to a reasonable formation/exchange rate and fortunately, the system is also consistent with a transition metal(II) extraction[20] at pD 2 to 3.5.

During the study of dynamic reactions in biphasic systems, the determination of the concentrations of each compound in each phase is essential to understand where the reaction takes place and to follow the redistributions of reactants (Fig. S32–S36 in ESI†). A vigorous stirring is necessary as the components/constituents interact only through the interface between the two phases. The stirring of the mixture ensures a large surface area of contact between the two immiscible phases and thus a high rate of molecular transfer between them.

Comparing the mono and biphasic systems, the acylhydrazone formation is significantly slower in the biphasic system than in a single-phase system except at the lowest pD (Tables 1a and 2a). The exchange reaction between **HA1B1** and **B2** is also faster in the aqueous medium itself but is nevertheless fast enough to reach equilibrium in the biphasic system at a timescale (10 hours) suitable for performing the liquid–liquid extraction.

Complexation of Cu(II) nitrate by acylhydrazones

Efficient extraction of Cu(II) ions by acylhydrazones in a biphasic system is dependent on the complexation of metal cation by the ligand. To this end, the coordination properties of the Cu(II) cation with the acylhydrazone **HA1B1** were investigated through single-crystal structure determinations. As the acylhydrazones N–H present a labile proton, three complexes of different charges, 2^+, 1^+ and neutral, may be formed between a Cu(II) cation and two tridentate **HA1B1** ligands depending on the ligand ionization: respectively [Cu(II)(**HA1B1**)$_2$](NO$_3$)$_2$ (type 1), [Cu(II)(**HA1B1**)(**A1B1**)](NO$_3$) (type 2), and [Cu(II)(**A1B1**)$_2$] (type 3). In view of their potential biological applications, the [Cu(acylhydrazone)$_n$] complexes have been extensively studied and the structures of all three types of complexes have been reported.[21]

Single crystals of [Cu(II)(**HA1B1**)$_2$](NO$_3$)$_2$ and [Cu(II)(**HA1B1**)(**A1B1**)](NO$_3$) were obtained and their molecular structures determined by X-ray crystallography (Fig. 3 and S37, Table S2 in ESI†). For [Cu(II)(**A1B1**)$_2$] (type 3), we have tested different conditions for crystal growth to obtain suitable crystals but unfortunately only chain polymers of [–Cu(L$^-$)$_2$–CuCl$^-$]$_n$ type had been obtained (Fig. S37 and Table S3 in ESI†).

The earlier structural studies[21] of complexes of types 1 and 2 involved anions other than nitrate but no significant differences from the present are apparent. In both present cases, the nitrate ions are in the second coordination sphere and form hydrogen bonds with the N–H sites of the acylhydrazone ligands, contributing to the overall stabilization of the crystal lattice. Both complexes have a strongly deformed octahedral coordination geometry (Fig. S37 and Table S4 in ESI†). The trans bonds show large deviation from 180°, with the following angles: N^4–Cu–O^2: 156.5° and N^1–Cu–O^1: 147° for complex 1; and 156.7° and 145.6° for complex 2. Comparison between (type 1) and (type 2) complexes, especially the shortening of one of the O–Cu bonds from over 2.1 Å to about 2 Å, indicates the deprotonation of one ligand out of two favours the enol-imine form over the keto-amine form of the protonated ligand left. This is in line with a shortening of the OC–N bond and a lengthening of NC–O. This structural feature is strongly dependent on the NH–X hydrogen bond, type 1: X = NO$_3^-$ and type 2: X = N$^-$ site of another complex (Fig. S38 in ESI†).

Extraction properties of components and constituents

The extraction properties of the components **A1**, **B1**, **B2** and the constituents **HA1B1** and **HA1B2** were first studied in the presence of copper(II) nitrate in a H$_2$O : CHCl$_3$ (v/v, 1 : 1) biphasic system by spectrophotometry and by direct Cu analysis using inductively coupled plasma optical emission spectrometry (ICP-OES; Fig. S39 and S40 in ESI†). At pH = 4.4, **A1**, **B1** and **HA1B1** did not extract Cu(II) ions, whereas **B2** and **HA1B2** showed promising properties, extracting respectively 60 ± 2% and 45 ± 1% of Cu(II) into the organic phase (Fig. S39 and S45, Tables S5–S10 in ESI†).

Further liquid–liquid extraction studies on **B2** and **HA1B2** separately showed that pH (2 to 5) and stirring time (5 to 900 min) had a limited effect on the phase transfer process (Tables S5–S10 in ESI†). When the amount of Cu(II) increased from 0.05 to 0.5 equiv. with respect to 1 equiv. of **HA1B2** ligand, the fraction of extracted cation decreased. On the other hand, the fraction extracted by **B2** increased between 0.05 to 0.25 equivalent of Cu(II) and then decreased slightly at 0.5 equivalent (Fig. S40 in ESI†).

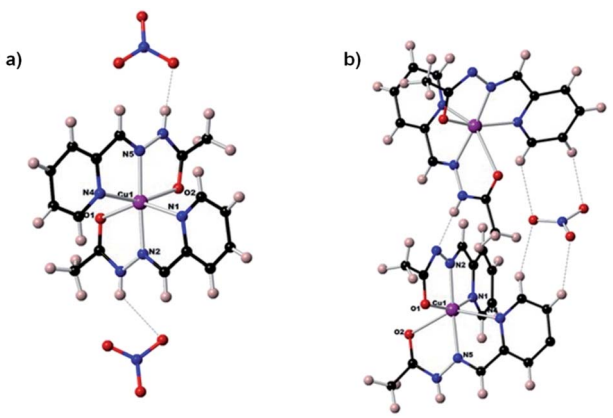

Fig. 3 Molecular structures of the complexes (a) [Cu(II)(**HA1B1**)$_2$](NO$_3$)$_2$ (Type 1) (b) [Cu(II)(**HA1B1**)(**A1B1**)](NO$_3$) (Type 2).

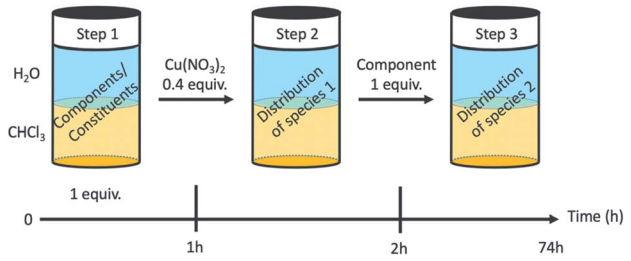

Fig. 4 Dynamic extraction procedure.

Table 3 Dynamic extraction experiments by the [A1 + B1 + B2] system (20 mM each in D_2O : $CDCl_3$ at pD = 3 and 296 K)

Extraction	Step 1	Step 2	Step 3	Efficiency (% of Cu in $CDCl_3$)
I	**HA1B1**	Cu(II)	**B2**	41%
II	**A1** + **B1**	Cu(II)	**B2**	42%
III	**A1** + **B1** + **B2**	Cu(II)	—	43%
Reverse	**HA1B2**	Cu(II)	**B1**	32%

Dynamic component exchange enabling metal phase transfer

The dynamic behaviour of the DCL of components **A1**, **B1**, **B2** in the presence of Cu(II) was investigated by different experiments involving 2 or 3 steps. A typical experiment consisted of starting with two initial components, followed by the addition of copper(II) nitrate and thereafter the third component (Fig. 4 and Section 8 of ESI†).

Four different extraction experiments were performed (Table 3), designed to determine the behaviour of both components and constituents independently. The main issue was the determination of the speciation of the library in each phase, using ICP-OES, NMR spectroscopy (after Cu(II) precipitation) and mass spectrometry to characterise and quantify the system. In order to compare the different experiments, the steps 1 and 2 were conducted over 1 hour (except for extraction III). The final step (the step 2 for extraction III) was left to equilibrate for up to 72 h. In all cases, the pD was around 3 (2.8 to 3.5).

Extraction experiment I

Step 1. This first experiment deals with the behaviour of the **HA1B1** constituent in the presence of Cu(II) and the **B2** component. In the biphasic set-up, the acylhydrazone **HA1B1** gives the previously observed distribution ratio of 43 : 56 (D_2O : $CDCl_3$) with an amount of hydrolysis below the detection limit (5%) (Fig. 5a and S60, Tables S12, S13 in ESI†).

Step 2. In the second step, the 0.4 equivalents of added Cu(II) remained in the aqueous phase (99%) (Fig. 5b). Transfer of **HA1B1** from the organic phase to the aqueous phase did occur, resulting in an equilibrium distribution of 19% of free **HA1B1** and 78% of [Cu(**HA1B1**)$_2$(II)]$(NO_3)_2$ presents in the water phase (Fig. 5a; S61–S64 and Tables S12, S13, S18, S19 in ESI†).

Step 3. In the third step, 1.0 equivalent of the lipophilic hydrazide **B2** component was added and the evolution of the system was followed over time until it stabilized after about 3 days (Fig. 5a, S65, S67 and Tables S12, S13, S18, S19 in ESI†). After three days of stirring, 41% Cu(II) was extracted into the $CDCl_3$ phase and the specie mainly (see hereafter) extracted was [Cu(II)(**HA1B2**)(**A1B2**)](NO_3). The form of this complex was determined indirectly as no crystal is obtained directly from the organic phase. Mass spectra exhibit the isotopic pattern of a complex containing one Cu coordinated to 2 molecules of **HA1B2**. The protonation state of the ligands was ascertained by quantifying the amount of nitrate counter-anion present in the organic phase. Thus, considering that Cu is doubly charged and that the species must be neutral to transfer to chloroform, the determination of the Cu : NO_3 ratio in chloroform gives access to the number of deprotonated ligands. Five hours after the addition of **B2**, the ratio was 0.5, meaning that two nitrate anions were extracted with the complex and thus that the two ligands were protonated (**HA1B2**). At thermodynamic equilibrium after 70 h, the ratio was 0.8, indicating that one of the two ligands had slowly and partially deprotonated (with liberation of the elements of nitric acid transferred into the water phase) leading to the formation of the complex as [Cu(II)(**HA1B2**)(**A1B2**)](NO_3) (Fig. 5c, Scheme 3).

In the aqueous phase, the total amount of copper(II) was 59% (Fig. 5b). The species containing copper(II) were found to be [Cu(II)(**HA1B1**)$_2$]$(NO_3)_2$ (19%), [Cu(II)(**B1**)$_2$]$(NO_3)_2$ (25%) and [Cu(II)(**HA1B1**)(**HA1B2**)]$(NO_3)_2$ (2%). The concentration of free **B1** in water increased over time up to 12%. Conversely, **HA1B1** decreased in the aqueous phase to release free **A1** that transferred to the chloroform phase and reacted with **B2** to form **HA1B2**. In these changes resides the operation of the dynamic extraction process.

Taken together, the addition of the hydrophobic component **B2** into the organic phase led to a reaction with the hydrophilic complex [Cu(II)(**HA1B1**)$_2$]$(NO_3)_2$. The reactions occurs between the two phases and induces the transfer of Cu(II) from the aqueous phase to the organic phase in the form of the [Cu(II)(**HA1B2**)$_2$]$(NO_3)_2$ and [Cu(II)(**HA1B2**)(**A1B2**)](NO_3) complexes. The occurrence of the covalent dynamic **B1**/**B2** component exchange determines the Cu(II) extraction capability of the process.

Extraction experiment II

Step 1. According to the general procedure, the two components **A1** and **B1** (1 equiv. each) were introduced into the biphasic system. The system was stirred for one hour at pD = 5 and the free **HA1B1** constituent obtained (72%) was found to be distributed between the two phases in the ratio 1 : 2 (aqueous : organic). The same occurred for the remaining free **A1** and **B1** (Fig. 5d; Tables S14 and S15 in ESI†).

Step 2. Although the formation of **HA1B1** was not complete, we decided to follow the same protocol for all the experiments to be able to compare them. Thus, 0.4 equiv. of copper(II) nitrate was added one hour after the beginning of the experiment. It induced a redistribution of the components and the constituents. 98% of Cu(II) remained in the water phase and mainly formed the complex [Cu(II)(**HA1B1**)$_2$]$(NO_3)_2$ (Fig. 5e; Tables S14, 15, S18, S19 in ESI†).

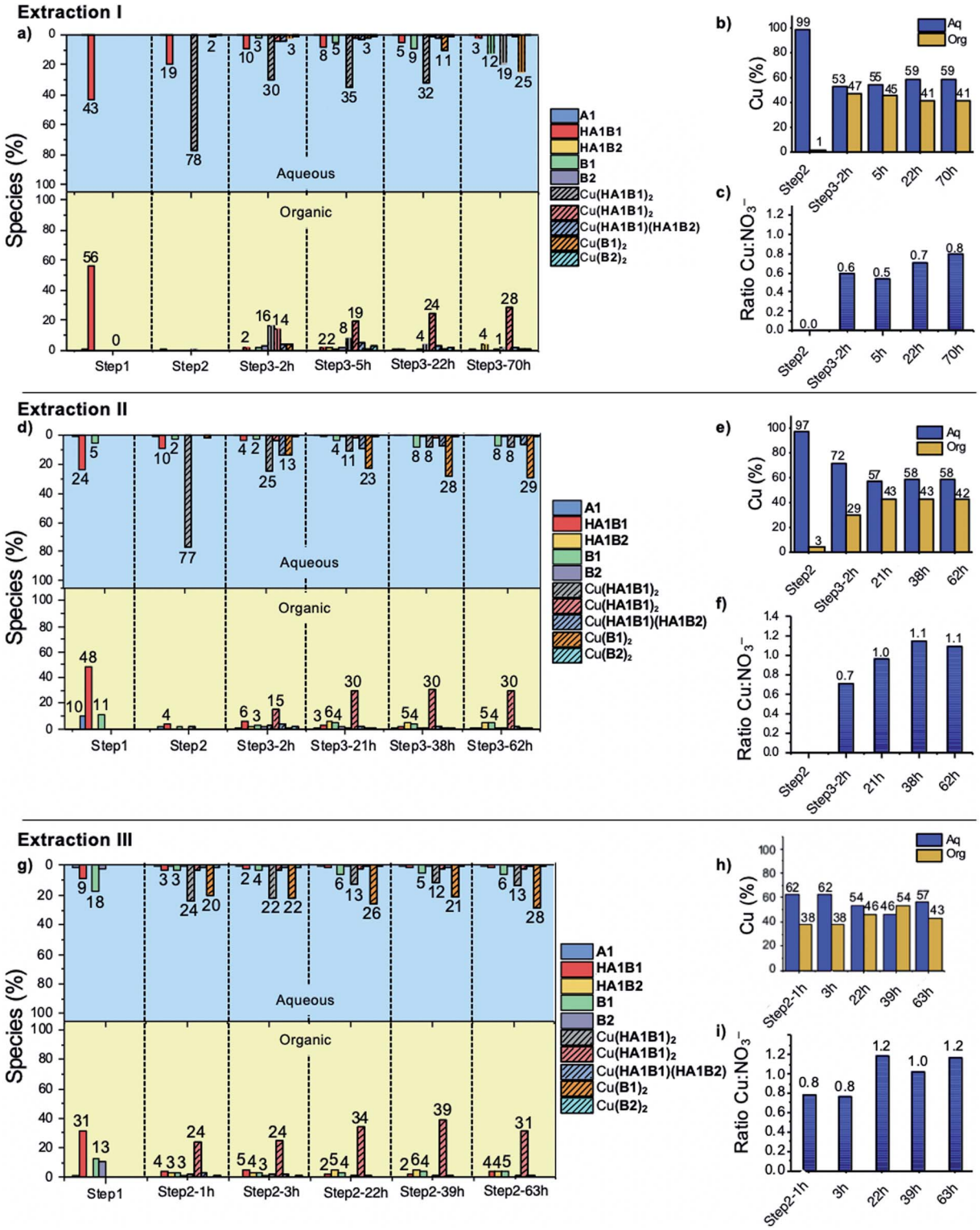

Fig. 5 Extraction I (a) distribution (%) of species between the two phases (b) distribution (%) of Cu(II) in each phase (c) molar Cu : NO_3 ratio in chloroform phase – extraction II (d) distribution (%) of species between the two phases (e) distribution (%) of Cu(II) in each phase (f) molar Cu : NO_3 ratio in chloroform phase – extraction III (g) distribution (%) of species between the two phases (h) distribution (%) of Cu(II) in each phase (i) molar Cu : NO_3 ratio in chloroform phase.

Step 3. One hour later, 1.0 equiv. of the lipophilic hydrazide component **B2** was introduced. The system evolved until reaching equilibrium after 21 h of stirring. The composition of the organic phase was then close to that observed in extraction I, with 42% of the Cu(II) extracted into the $CDCl_3$ phase. The Cu : NO_3 ratio was 1 : 1 which means that the acylhydrazone

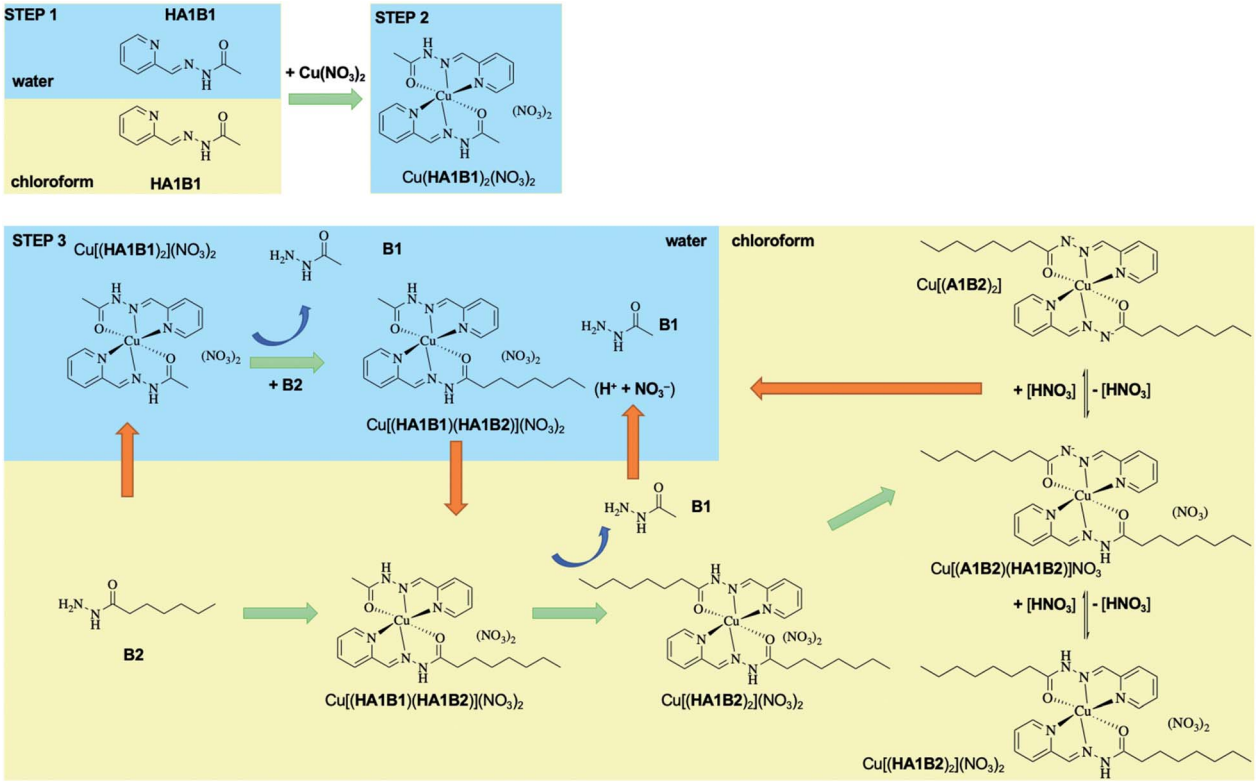

Scheme 3 Proposed mechanism of the covalent dynamic Cu(II) extraction from water to chloroform operating through dynamic covalent extracting agents along the sequence of steps followed in the extraction experiment I above. Only the main species are represented.

complex species are on the average monodeprotonated, the most abundant (30%) being [Cu(II)(**HA1B2**)(**A1B2**)](NO$_3$) (Fig. 5f; Tables S14, S15, S18, S19 in ESI†). The final state of the water phase composition displays roughly the same histogram signature as for extraction I, which means that even if the intermediate steps (1 and 2) were not completely at equilibrium, the system finally reached thermodynamic equilibrium.

Extraction experiment III

Step 1. Finally, an experiment was conducted starting with an initial mix of all components of the library. Unlike previous extraction experiments, it took place in two steps. First, the components **A1**, **B1** and **B2** were introduced in equimolar amounts in the biphasic system at the initial pD of 5.6. As previously observed, the reaction was slow, giving after one hour 31% of **HA1B1** in chloroform and 9% in water together with 14% **HA1B2** in chloroform. The components left free were distributed over both two phases (Fig. 5g; Tables S16, S17 in ESI†).

Step 2. Then, Cu(NO$_3$)$_2$ (0.4 equiv.) was added and the evolution was followed over 3 days. The final copper extraction yield in chloroform was 43% and remained rather stable between 2 h and 3 days of stirring. In the organic phase, the formation of [Cu(II)(**HA1B2**)(**A1B2**)](NO$_3$) was favoured and reached 31% (Fig. 5g and h; Tables S16–S19 in ESI†). The water phase contained [Cu(II)(**HA1B1**)$_2$](NO$_3$)$_2$ and [Cu(II)(**B1**)$_2$](NO$_3$)$_2$ both at 22% after 2 h. After 3 days, their proportions were respectively 13% and 28%. The total amount of coordinated species remained stable. Free **B1** (6%) was present as well as small amounts (1–2%) of the organic species **A1**, **HA1B1** and **B2** (Fig. 5g; Tables S16–S19 in ESI†).

As in previous extractions, the comparison of the histogram signatures shows that the final state of the chloroform phase is very close to that of the other extraction experiments.

Global discussion of the extraction experiments

All three extraction experiments described above led to almost the same distribution of Cu(II) between the aqueous and the organic phases. They converge to a common final histogram signature after different sequences of additions/exchanges leading to a partial extraction of Cu(II).

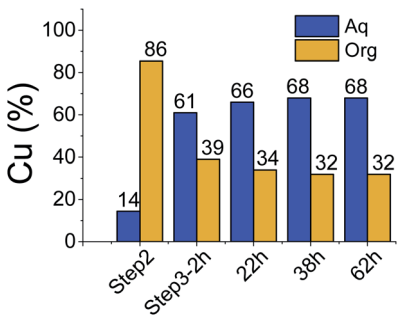

Fig. 6 Distribution (%) of Cu(II) in each phase in the reverse experiment.

A simplified experiment, starting from **HA1B2** and forming [Cu(II)(**HA1B2**)(**A1B2**)](NO_3) in chloroform after copper(II) nitrate (0.4 equiv.) addition, showed that subsequent addition of **B1** (1.0 equiv.) triggered the transfer of Cu(II) from the chloroform to the aqueous phase by forming hydrophilic complexes (Fig. 6; Table S20 in ESI†).

This experiment demonstrates the complete reversibility of the extraction process.

The present dynamic studies have shown that it is possible to transfer Cu(II) from an aqueous phase to an organic phase or from an organic phase to an aqueous phase using the adaptive properties of a 3-component dynamic covalent library (Scheme 3).

The in-depth analytical study of the species and their behaviour over time provides the data for deriving the pathways and entities of the extraction mechanism for Cu(II) phase transfer (Scheme 3, Fig. S68 in ESI†). The analyses show a complicated evolution of the interactions between Cu(II) and the constituents **HA1B1** and **HA1B2**. To some extent, Cu(II) also interacts with the components **B1** and **B2**.

The main pathway leading to Cu(II) extraction by the present process involving dynamic covalent extracting agents may be considered to occur in 4 steps.

(1) The addition of the Cu(II) nitrate to the constituent **HA1B1** in a biphasic D_2O : $CDCl_3$ set-up leads to the formation of [Cu(II)(**HA1B1**)$_2$](NO_3)$_2$ in the aqueous phase only.

(2) The lipophilic **B2** added thereafter reacts with [Cu(II)(**HA1B1**)$_2$](NO_3)$_2$ through the interface by an acid-catalysed exchange reaction. In the first instance, [Cu(II)(**HA1B1**)(**HA1B2**)](NO_3)$_2$ is produced and distributed in both phases. **B1** is released mainly into the aqueous phase and forms a small amount of [Cu(II)(**B1**)$_2$](NO_3)$_2$ in water.

(3) As a result of the **B1**/**B2** exchange, [Cu(II)(**HA1B2**)$_2$](NO_3)$_2$ is produced and passes preferentially into the organic phase. The small amount of residual **B2** produces a little [Cu(II)(**B2**)$_2$](NO_3)$_2$ complex in chloroform.

(4) Finally, in chloroform, the [Cu(II)(**HA1B2**)$_2$](NO_3)$_2$ complex by releasing the elements of nitric acid (that rapidly transfers to the aqueous phase) generates an equilibrium mixture of three complexes in different states of protonation [Cu(II)(**HA1B2**)$_2$](NO_3)$_2$, [Cu(II)(**HA1B2**)(**A1B2**)](NO_3) and [Cu(II)(**A1B2**)$_2$]. The overall process is thermodynamically driven by the deprotonation of the ligand through the increase in N–H acidity resulting from Cu(II) complexation (Scheme 3).

Conclusions

The present work achieves the liquid–liquid extraction of copper(II) cations by means of a dynamic covalent library performing adaptation through reversible component exchange. It provides a detailed analysis of the ability of a DCL of acylhydrazones to complex and transfer copper(II) cations from an aqueous phase to an organic chloroform phase by the generation of a DCL of ligands through component exchange across the interface of the two-phase system. The final constituents of the library strongly coordinate the metal ions and the lipophilic acylhydrazone ligand generated enables the metal extraction. The addition of the metal salt to the DCL induces a dynamic covalent reshuffling of the system. The different ways used to obtain the dynamic library lead to the same thermodynamic equilibrium distribution of entities after copper addition showing the reversibility of the process. Finally, studying the reversibility and the adaptability of the system provides some understanding of the mechanism of extraction. However, the analytical investigations show both the novel possibilities offered and the complicated behaviour introduced by the use of DCC in liquid–liquid extraction methodologies. The versatility of the approach paves the way to more complex systems both from a dynamic library point of view and from that of metal ion extraction/separation processes, which may be made selective by suitable choice of the components of the DCL.

Conflicts of interest

There are no conflicts to declare.

Acknowledgements

The authors thank the ERC (Advanced Research Grant SUPRADAPT 290585), the ANR Grant DYNAFUN as well as the University of Strasbourg Institute for Advanced Study (USIAS) and the Commissariat à l'Énergie Atomique et aux Énergies Alternatives (CEA) for financial support. AC thanks the CEA for a doctoral fellowship, Pr. Jack Harrowfield for discussions, Dr Jean-Louis Schmitt, Cyril Antheaume and Dr Bruno Vincent for helpful discussions of NMR and HRMS data as well as Corinne Bailly, and Dr Lydia Karmazin for the X-ray crystallographic structure determinations. AC thanks Dr Anne Boos, Ilsah El Masoudi and Pascale Ronot for ICP-AES analyses.

Notes and references

‡ Researchers and engineers working in the field of liquid–liquid separation define the solvent as a combination of a diluent, an extractant and sometimes, additional molecules often called co-extractant. In the present context, the term of solvent used corresponds to the diluent.

§ The notation **AaBb** designates a deprotonated acylhydrazone group with a site N^-.

1 (*a*) V. Manchanda and P. Pathak, *Sep. Purif. Technol.*, 2004, **35**, 85–103; (*b*) D. Whittaker, A. Geist, G. Modolo, R. Taylor, M. Sarsfield and A. Wilden, *Solvent Extr. Ion Exch.*, 2018, **36**, 223–256; (*c*) K. Kiegiel, L. Steczek and G. Zakrzewska-Trznadel, *Journal of Chemistry*, 2013, 762819; (*d*) Y. Morita, Y. Sasaki, T. Asakura, Y. Kitatsuji, Y. Sugo and T. Kimura, *IOP Conf. Ser.: Mater. Sci. Eng.*, 2010, **9**, 012057; (*e*) E. Aneheim, B. Grüner, C. Ekberg, M. Foreman, Z. Hájková, E. Löfström-Engdahl, M. Drew and M. Hudson, *Polyhedron*, 2013, **50**, 154–163; (*f*) A. Mudring and S. Tang, *Eur. J. Inorg. Chem.*, 2010, **18**, 2569–2581; (*g*) M. Alyapyshev, V. Babain and Y. Ustynyuk, *Russ. Chem. Rev.*, 2016, **85**, 943–961; (*h*) P. Baron, S. Cornet, E. Collins, G. DeAngelis, G. Del Gul, Y. Fedorov, H. Glatz, V. Ignatiev, T. Inoue, A. Khaperskaya, I. Kim, M. Kormilitsyn, T. Koyama, J. Law, H. Lee, K. Minato, Y. Morita, J. Uhlíř, D. Warin and R. Taylor, *Prog. Nucl. Energy*, 2019, **117**, 103091.

2 (*a*) T. Lasheen, M. El-Ahmady, H. Hassib and A. Helal, *Miner. Process. Extr. Metall. Rev.*, 2015, **36**, 145–173; (*b*) Y. El-Nadi, *Sep. Purif. Rev.*, 2017, **46**, 195–215; (*c*) T. Nguyen and M. Lee, *Miner. Process. Extr. Metall. Rev.*, 2019, **40**, 265–277; (*d*) N. Hidayah and S. Abidin, *Miner. Eng.*, 2018, **121**, 146–157; (*e*) A. Deep and J. De Carvalho, *Solvent Extr. Ion Exch.*, 2008, **26**, 375–404.

3 (*a*) T. Nguyen and M. Lee, *Miner. Process. Extr. Metall. Rev.*, 2019, **40**, 278–291; (*b*) A. Paiva, *Solvent Extr. Ion Exch.*, 2000, **18**, 223–271; (*c*) M. Jha, V. Kumar, J. Jeong and J. Lee, *Hydrometallurgy*, 2012, **111–112**, 1–9; (*d*) A. Agrawal, S. Kumari and K. Sahu, *Ind. Eng. Chem. Res.*, 2009, **48**, 6145–6161; (*e*) G. Cote, *Solvent Extr. Ion Exch.*, 2000, **18**, 703–727; (*f*) M. Jha, D. Gupta, J. Lee, V. Kumar and J. Jeong, *Hydrometallurgy*, 2014, **142**, 60–69; (*g*) M. Jha, A. Kumari, R. Panda, J. Rajesh Kumar, K. Yoo and J. Lee, *Hydrometallurgy*, 2016, **161**, 77–101; (*h*) N. Swain and S. Mishra, *J. Cleaner Prod.*, 2019, **220**, 884–898; (*i*) F. Mary, G. Arrachart, A. Leydier and S. Pellet-Rostaing, *Tetrahedron*, 2019, **75**, 3968–3976; (*j*) M. Toure, G. Arrachart, J. Duhamet and S. Pellet-Rostaing, *Metals*, 2018, **8**, 1–11; (*k*) L. Wang and M. Lee, *J. Ind. Eng. Chem.*, 2016, **39**, 1–9.

4 (*a*) R. Poirot, X. Le Goff, O. Diat, D. Bourgeois and D. Meyer, *ChemPhysChem*, 2016, 2112–2117; (*b*) W. Zoubi, *J. Coord. Chem.*, 2013, **66**, 2264–2289; (*c*) A. Grilo, M. Aires-Barros and A. Azevedo, *Sep. Purif. Rev.*, 2016, **45**, 68–80; (*d*) N. Zhou and J. Wu, *Prog. Nat. Sci.*, 2003, **13**, 1–12; (*e*) E. Werner and S. Biros, *Inorg. Chem. Front.*, 2019, **6**, 2067–2094; (*f*) K. Omelchuk, M. Stambouli and A. Chagnes, *J. Mol. Liq.*, 2018, **262**, 111–118; (*g*) B. Braibant, X. Le Goff, D. Bourgeois and D. Meyer, *ChemPhysChem*, 2017, **18**, 3583–3594; (*h*) A. Leoncini, J. Huskens and W. Verboom, *Chem. Soc. Rev.*, 2017, **46**, 7229–7273; (*i*) T. Sukhbaatar, S. Dourdain, R. Turgis, J. Rey, G. Arrachat and S. Pellet-Rostaing, *Chem. Commun.*, 2015, **51**, 15960–15963; (*j*) M.-C. Dul, B. Braibant, S. Dourdain, S. Pellet-Rostaing, D. Bourgeois and D. Meyer, *J. Fluorine Chem.*, 2017, **200**, 59–65; (*k*) Y. Liu, M. Lee and G. Senanayake, *J. Mol. Liq.*, 2018, **268**, 667–676; (*l*) R. Srivastava, J.-C. Lee and M.-S. Kim, *J. Chem. Technol. Biotechnol.*, 2015, **90**, 1752–1764; (*m*) M. Špadina, K. Bohinc, T. Zemb and J.-F. Dufrêche, *Langmuir*, 2019, **35**, 3215–3230; (*n*) T. Zemb, C. Bauer, P. Bauduin, L. Belloni, C. Déjugnat, O. Diat, V. Dubois, J.-F. Dufrêche, S. Dourdain, M. Duvail, C. Larpent, F. Testard and S. Pellet-Rostaing, *Colloid Polym. Sci.*, 2014, **293**, 1–22.

5 (*a*) J.-M. Lehn, *Chem.–Eur. J.*, 1999, **5**, 2455–2463; (*b*) J.-M. Lehn, *Chem. Soc. Rev.*, 2007, **36**, 151–160; (*c*) J.-M. Lehn, *Angew. Chem., Int. Ed.*, 2013, **52**, 2836–2850; (*d*) S. Rowan, S. Cantrill, G. Cousins, J. Sanders and J. Stoddart, *Angew. Chem., Int. Ed.*, 2002, **41**, 898–952; (*e*) P. Corbett, J. Leclaire, L. Vial, K. West, J.-L. Wietor, J. Sanders and S. Otto, *Chem. Rev.*, 2006, **106**, 3652–3711; (*f*) Y. Jin, C. Yu, R. Denman and W. Zhang, *Chem. Soc. Rev.*, 2013, **42**, 6634–6654.

6 (*a*) G. Vantomme, S. Jiang and J.-M. Lehn, *J. Am. Chem. Soc.*, 2014, **136**, 9509–9518; (*b*) J. Holub, G. Vantomme and J.-M. Lehn, *J. Am. Chem. Soc.*, 2016, **138**, 11783–11791; (*c*) S. Dhers, J. Holub and J.-M. Lehn, *Chem. Sci.*, 2017, **8**, 2125–2130; (*d*) J. Klein, V. Saggiomo, L. Reck, U. Lüning and J. Sanders, *Org. Biomol. Chem.*, 2012, **10**, 60–66.

7 (*a*) G. Men and J.-M. Lehn, *J. Am. Chem. Soc.*, 2017, **139**, 2474–2483; (*b*) G. Men and J.-M. Lehn, *Chem. Sci.*, 2019, **10**, 90–98.

8 (*a*) J. Armao and J.-M. Lehn, *J. Am. Chem. Soc.*, 2016, **138**, 16809–16814; (*b*) M. He and J.-M. Lehn, *J. Am. Chem. Soc.*, 2019, **141**, 18560–18569.

9 (*a*) N. Hafezi and J.-M. Lehn, *J. Am. Chem. Soc.*, 2012, **134**, 12861–12868; (*b*) G. Vantomme, N. Hafezi and J.-M. Lehn, *Chem. Sci.*, 2014, **5**, 1475–1483.

10 J.-M. Lehn, *Angew. Chem., Int. Ed.*, 2015, **54**, 3276–3289.

11 A. Osypenko, S. Dhers and J.-M. Lehn, *J. Am. Chem. Soc.*, 2019, **141**, 12724–12737.

12 (*a*) D. Epstein, s. Choudhary, M. R. Churchill, K. Keil, A. Eliseev and J. Morrow, *Inorg. Chem.*, 2001, **40**, 1591–1596; (*b*) S. Choudhary and J. Morrow, *Angew. Chem., Int. Ed.*, 2002, **41**, 4096–4098.

13 X.-Q. Chen, Y.-D. Cai, W. Jiang, G. Peng, J.-K. Fang, J.-L. Liu, M.-L. Tong and X. Bao, *Inorg. Chem.*, 2019, **58**, 999–1002.

14 X. Su and I. Aprahamian, *Chem. Soc. Rev.*, 2014, **43**, 1963–1981.

15 (*a*) A. Ekström, J. Wang, J. Bella and D. Campopiano, *Org. Biomol. Chem.*, 2018, **16**, 8144–8149; (*b*) S. Ulrich, *Acc. Chem. Res.*, 2019, **52**, 510–519.

16 J. Wyman and E. Ingalls, *J. Am. Chem. Soc.*, 1938, **60**, 1182–1184.

17 (*a*) E. Cordes and W. Jencks, *J. Am. Chem. Soc.*, 1962, **84**, 832–837; (*b*) D. Larsen, A. Jeppesen, C. Kleinlein and M. Pittelkow, *Chem. Sci.*, 2018, **9**, 5252–5259; (*c*) M. Ciaccia, S. Pilati, R. Cacciapaglia, L. Mandolini and S. Di Stefano, *Org. Biomol. Chem.*, 2014, **12**, 3282–3287.

18 D. Kölmel and E. Kool, *Chem. Rev.*, 2017, **117**(15), 10358–10376.

19 A. L. Horvath and F. W. Getzen, *IUPAC Solubility Data Series*, 1995, vol. 60.

20 (*a*) D. Peppard, *Advances in Inorganic Chemistry and Radiochemistry*, ed. H. J. Emeléus and A. G. Sharpe, 1966, pp. 1–80; (*b*) Y. Marcus, *Solvent extraction of inorganic species*, American Chemical Society, 1963; (*c*) C. Cheng, *Hydrometallurgy*, 2006, **84**, 109–117; (*d*) A. Nayl, M. Hamed and S. Rizk, *J. Taiwan Inst. Chem. Eng.*, 2015, **55**, 119–125.

21 (*a*) R. Patel, Y. P. Singh, Y. Singh, R. Butcher, M. Zeller, R.-K. Singh and O. U-Wang, *J. Mol. Struct.*, 2017, **1136**, 157–172; (*b*) M. Angelusiu, S.-F. Barbuceanu, C. Draghici and G. Almajan, *Eur. J. Med. Chem.*, 2010, **45**, 2055–2062; (*c*) C. Armstrong, P. Bernhardt, P. Chin and D. Richardson, *Eur. J. Inorg. Chem.*, 2003, **6**, 1145–1156; (*d*) Y. Du, W. Chen, X. Fu, H. Deng and J. Deng, *RSC Adv.*, 2016, **6**, 109718–109725; (*e*) J. Deng, Y. Gou, W. Chen, X. Fu and H. Deng, *Bioorg. Med. Chem.*, 2016, **24**, 2190–2198; (*f*) R. Patel, Y. Singh, Y. P. Singh, R. Butcher, A. Kamal and I. Tripathi, *Polyhedron*, 2016, **117**, 20–34; (*g*) Y. P. Singh, R. Patel, Y. Singh, R. Butcher, P. Vishakarma and R. K. Singh, *Polyhedron*, 2017, **122**, 1–15.